RESEARCH ARTICLE

WILEY

Oscillatory and structural signatures of language plasticity in brain tumor patients: A longitudinal study

Lucia Amoruso[1,2] | Shuang Geng[1,3] | Nicola Molinaro[1,2] | Polina Timofeeva[1,3] |
Sandra Gisbert-Muñoz[1,3] | Santiago Gil-Robles[4,5] | Iñigo Pomposo[5] |
Ileana Quiñones[1] | Manuel Carreiras[1,2,3]

[1]Basque Center on Cognition, Brain and Language (BCBL), San Sebastian, Spain

[2]IKERBASQUE, Basque Foundation for Science, Bilbao, Spain

[3]University of the Basque Country, UPV/EHU, Bilbao, Spain

[4]Department of Neurosurgery, Hospital Quiron, Madrid, Spain

[5]BioCruces Research Institute, Bilbao, Spain

Correspondence
Lucia Amoruso, Basque Center on Cognition, Brain and Language (BCBL), 20009 San Sebastian, Spain.
Email: l.amoruso@bcbl.eu

Abstract

Recent evidence suggests that damage to the language network triggers its functional reorganization. Yet, the spectro-temporal fingerprints of this plastic rearrangement and its relation to anatomical changes is less well understood. Here, we combined magnetoencephalographic recordings with a proxy measure of white matter to investigate oscillatory activity supporting language plasticity and its relation to structural reshaping. First, cortical dynamics were acquired in a group of healthy controls during object and action naming. Results showed segregated beta (13–28 Hz) power decreases in left ventral and dorsal pathways, in a time-window associated to lexico-semantic processing ($\sim$250–500 ms). Six patients with left tumors invading either ventral or dorsal regions performed the same naming task before and 3 months after surgery for tumor resection. When longitudinally comparing patients' responses we found beta compensation mimicking the category-based segregation showed by controls, with ventral and dorsal damage leading to selective compensation for object and action naming, respectively. At the structural level, all patients showed preoperative changes in white matter tracts possibly linked to plasticity triggered by tumor growth. Furthermore, in some patients, structural changes were also evident after surgery and showed associations with longitudinal changes in beta power lateralization toward the contralesional hemisphere. Overall, our findings support the existence of anatomo-functional dependencies in language reorganization and highlight the potential role of oscillatory markers in tracking longitudinal plasticity in brain tumor patients. By doing so, they provide valuable information for mapping preoperative and postoperative neural reshaping and plan surgical strategies to preserve language function and patient's quality of life.

KEYWORDS
brain rhythms, brain tumors, language, magnetoencephalography, neuroplasticity

1 | INTRODUCTION

Neuroplasticity refers to the brain's ability to modify its structure and function throughout the lifespan, allowing the acquisition of new skills (Carreiras et al., 2009; Maguire et al., 2000) but also coping with brain damage and disease (Payne & Lomber, 2001). When considering this latter aspect, evidence from human studies in stroke (Butefisch et al., 2005; Shimizu et al., 2002) and brain tumor patients (Duffau, 2005; Robles, Gatignol, Lehericy, & Duffau, 2008) underscores the existence of different plasticity patterns, including function persistence within the tumor, function redistribution in perilesional areas, ipsilesional activation of more distant areas and recruitment of contralesional homologs. In line with a hodotopical understanding of brain organization (Catani, 2007; De Benedictis & Duffau, 2011; Duffau, Moritz-Gasser, & Mandonnet, 2014), functional reallocation would be possible thanks to the existence of redundant cortico–subcortical parallel networks potentially unmasked by the lesion. It has been suggested (Ius, Angelini, Thiebaut de Schotten, Mandonnet, & Duffau, 2011) that this high potential for reorganization would be almost confined to the cortical level, with subcortical white matter showing limited to null plasticity. Nonetheless, evidence from stroke (Schlaug, Marchina, & Norton, 2009) and epileptic patients following temporal lobectomy (Jeong, Asano, Juhasz, Behen, & Chugani, 2016; Li et al., 2019), suggests that white matter plasticity in the contralesional hemisphere is somehow possible.

Brain function and its reshaping in the damaged brain has been classically studied by means of functional magnetic resonance imaging (fMRI). However, hemodynamic responses are slow (one volume every ~2 s) and functions as language, which occur on the subsecond time-scale, need also to be examined with high-temporal resolution techniques capable of tracking linguistic processing in real-time. Electro- and magneto-encephalography (M/EEG) meet this requirement as they can capture neuronal activity and its oscillatory dynamics with millisecond time resolution, offering a new perspective to study brain plasticity (Reid et al., 2016).

Oscillations at different frequency-bands and their synchronization are thought to reflect communication within and between regions (Fries, 2005), relevant for behavior and disease (Uhlhaas et al., 2017). Recently, M/EEG studies have been successful in identifying oscillatory markers of brain damage and language recovery, underscoring the involvement of low-frequency activity in functional compensation. For instance, using MEG, Kielar, Deschamps, Jokel, and Meltzer (2016) reported the involvement of contralesional right alpha-beta activity during semantic processing in stroke patients. Similarly, Traut et al. (2019) found that brain tumor patients exhibited a functional shift in beta language lateralization toward the right hemisphere after left tumor resection. Using EEG, Spironelli, Manfredi, and Angrilli (2013) evaluated post-stroke language reorganization and found bilateral patterns of beta activity in ipsilesional frontal areas and contralesional homologs during semantic processing. Piai, Meyer, Dronkers, and Knight (2017) reported alpha–beta power decreases associated to lexico-semantic retrieval in stroke patients with left hemispheric lesions. Interestingly, while controls showed a left lateralized effect, patients exhibited a right lateralized one, which was ultimately predicted by the probability of splenium damage.

Here, we tracked oscillatory dynamics subserving language plasticity in brain tumor patients before and 3 months after surgery for tumor resection. We recorded MEG activity while healthy controls and patients overtly named object and action pictures in Spanish. Of note, brain tumors could affect either ventral or dorsal areas within the left hemisphere which are known to play different roles in representing object and action categories. Briefly, previous evidence (Gleichgerrcht et al., 2016; Lubrano, Filleron, Demonet, & Roux, 2014; Vigliocco, Vinson, Druks, Barber, & Cappa, 2011) suggests that the semantic processing of object and action knowledge is underpinned by partially distinct networks preferentially involving inferior-temporal and fronto-parietal nodes, respectively. Thus, we capitalized on this dissociation to evaluate language function in the healthy and the lesioned brain. Specifically, we expected different alpha-beta compensation patterns depending on tumor location and semantic category, with ventral and dorsal lesions mainly compromising object and action processing, respectively. We also expected that functional changes would be related to structural ones. Thus, we calculated a proxy measure of white matter involvement in language-related tracts and assessed if potential preoperative and/or postoperative structural reshaping was associated with functional longitudinal changes.

2 | MATERIALS AND METHODS

2.1 | Participants

A total of 26 participants took part in this study. Twenty healthy adults (6 men, age mean = 25.04; SD = 3.94) were recruited through the BCBL database and received economical compensation for their participation. Six patients (3 men, age range 24–59; mean = 40; SD = 12.89) with brain tumors in the left hemisphere mainly involving temporal (n = 3), fronto-parietal (n = 2) or parietal regions (n = 1) were recruited at the Cruces Hospital where they received their diagnosis and performed the awake craniotomy for tumor resection (see Figure 1 for lesion profile). One out of 6 patients had cavernous angiomas, while the other 5 exhibited astrocytomas Grade I and II. Individual patient demographics, lesion and clinical characteristics are summarized in Table 1. All participants were right handed as measured by Edinburgh Handedness Inventory (Oldfield, 1971). They all had normal hearing and normal or corrected to normal vision. All patients and controls reported Spanish as their first language and the average naming BEST score (de Bruin, Carreiras, & Duñabeitia, 2017) in Spanish was 63.17/65 for patients and 64.81/65 for controls. It should be noted, however, that patients and controls also reported knowing some Basque (40/65 for patients and 49/65 for controls), as is common in the population of Donostia-San Sebastian. The study protocol was approved by the Ethics Board of the Euskadi Committee and the Ethics and Scientific Committee of the BCBL, following the declaration of Helsinki. All participants gave their written consent prior to the study.
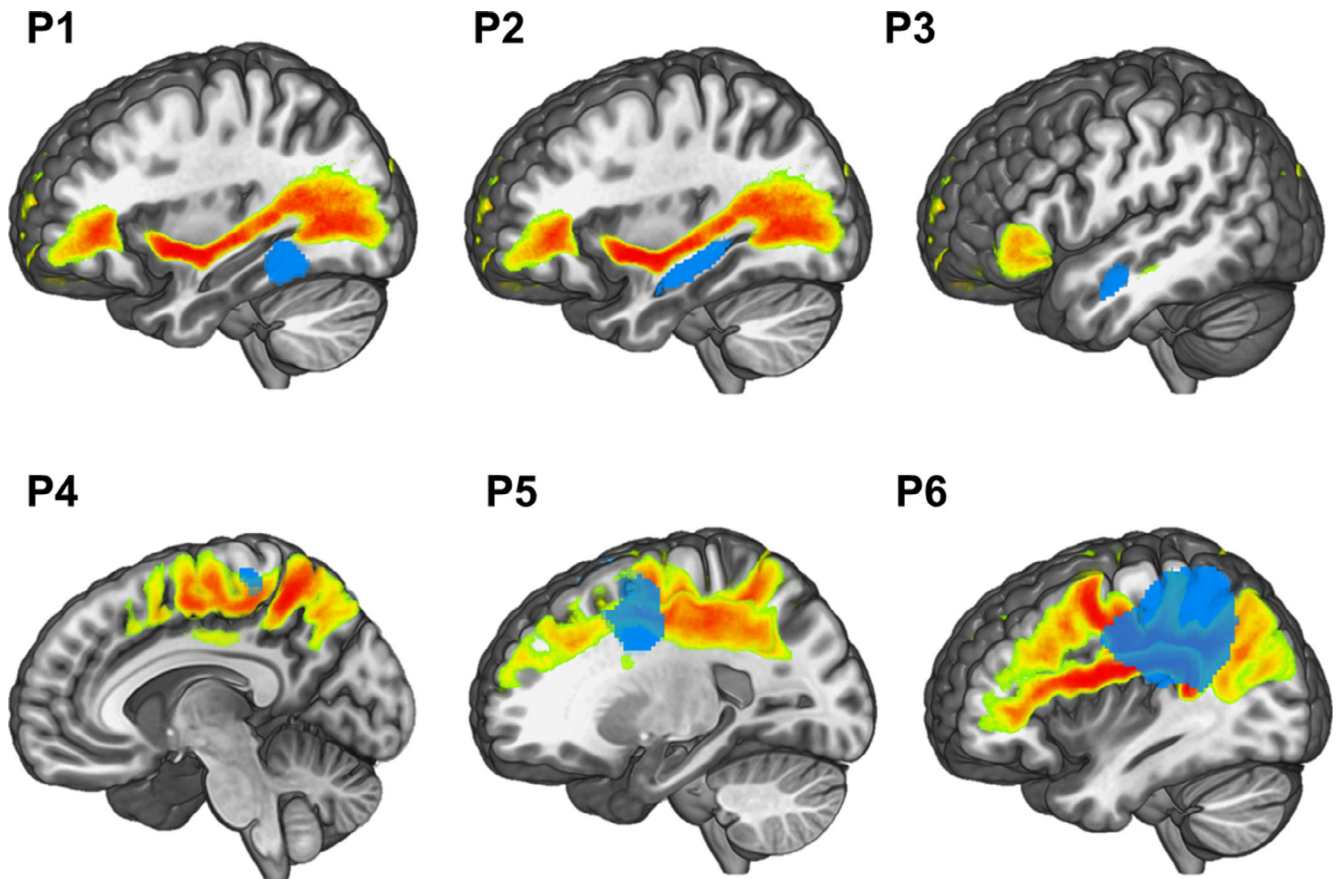
FIGURE 1 Lesion profile with respect to major dorsal and ventral white matter tracts. Tumors are shown in blue. Probabilistic location of superior longitudinal fasciculus (SLF, I, II), arcuate fasciculus (AF) and inferior fronto-occipital fasciculus (IFOF) are shown in orange. Patients 1, 2 and 3 (on top) exhibit tumors invading the left temporal lobe, however, none of them compromises the IFOF. Patients 4, 5, and 6 (on bottom) exhibit tumors invading fronto-parietal regions affecting, in all cases, the SLF and in cases 5 and 6 also the AF

TABLE 1 Demographics and clinical characteristics of patients

Patient ID	Age (years)	Gender	Education (years)	Handedness	Type of tumor	Tumor volume (cm^3)	Extent of resection (%)
P1	33	F	21	R	Cavernous Angioma	2.53	84.48
P2	59	M	12	R	Astrocytoma Grade II	5.8	100
P3	24	M	16	R	Astrocytoma Grade I	1.85	100
P4	46	F	14	R	Astrocytoma Grade II	0.55	75.83
P5	31	F	21	R	Astrocytoma Grade II	16.44	100
P6	47	M	19	R	Astrocytoma Grade II	74.25	100

2.2 | Stimuli and task

Semantic processing was assessed with a picture naming task. Pictures were selected from a standardized battery developed by NEURE clinic® (https://www.neure.eu/). The task included two separate sets of 30 colored images with line drawings either depicting objects or a person performing an action, respectively. Object and action stimuli were matched as close as possible for different linguistic variables and differences between stimuli were calculated using Student tests for normally distributed variables and Mann–Whitney for non-normally distributed ones. More specifically, stimuli were matched for frequency (Objects: mean = 25.94, SD = 29.19; Actions: mean = 14.79,

SD = 17.06, W = 562, p = .055), word length in terms of number of letters (Objects: mean = 5, SD = 1; Actions: mean = 6, SD = 1, t = −1.519, p = .13), and familiarity (Objects: mean = 6.26, SD = 0.5; Actions: mean = 6.17, SD = 0.56, t = 0.68, p = .49). Name agreement was ≥85% in both conditions.

In separate blocks, participants were requested to observe the pictures and name them overtly in Spanish. Production of nouns and verbs was requested in the context of short sentences, which is a more ecological form of speech than isolated naming. More specifically, on top of the object-related images we added the text "Esto es..." ["This is..." in Spanish] to force the production of a short sentence that had to agree in number with the target noun (e.g., "This is a bird", "This is an apple"). Similarly, on top of the action-related pictures, we included the pronouns "El..." or "Ella..." ["He..." or "She...", in Spanish]. This introductory text was used as a cue for the production of a sentence that started with the given subject and had a finite verb form in third person singular (e.g., "She sings," "He writes"). Importantly, the use of these pictures led to participants eliciting sentences comprising concrete nouns (i.e., as opposed to abstract concepts like "love") and dynamic motor actions (i.e., as opposed to verbs referring to static states like "thinking"). We used MatlabR2012B and Cogent Toolbox for picture presentation. Trials started with a fixation cross lasting for 500 ms, followed by the stimulus displayed for 1 s. ISI randomly varied between 2 and 4 s. Each picture was presented 3 times for a total of 90 trials per block. Each block lasted ~10 min, and participants were allowed to take a short break between them.

2.3 | Behavioral assessment

Vocal responses were recorded and monitored online by the experimenter while participants performed the task. Naming latencies were calculated using the Chronset tool (Roux, Armstrong, & Carreiras, 2017) which enables the automatic detection of speech onset. Responses containing disfluencies or errors were coded as invalid and excluded from MEG analysis. In addition, response latencies shorter than 200 ms and deviating from participant's mean latency by >2.5 SD in each condition (Miozzo, Pulvermuller, &

Hauk, 2015) were also removed (in total, ~5.9% of the trials were eliminated). Reaction times (RTs) and correct naming responses were compared between groups using nonparametric Welch's t-tests and Wilcoxon signed-rank for pre- versus post-surgery stages within the patient's group (see Table 2). Furthermore, we also ran Crawford-Howell (1998) frequentist t-tests for single-case analysis using the psycho Package (Makowski, 2018) on RStudio (Version 1.2.5019) to compare each patient to the control group (see Table 3).

2.4 | MEG and MRI acquisition

MEG data were acquired in a magnetically shielded room using a 360-channel Elekta-Neuromag system (Helsinki, Finland). Eye-movements were monitored with two pairs of electrodes in a bipolar montage placed on the external chanti of each eye (horizontal EOG) and above and below right eye (vertical EOG). Electrocardiographic (ECG) activity was also recorded with two electrodes, one positioned just below the right clavicle and the other below the left rib bone. MEG signals were continuously recorded at a 1 kHz sampling rate and on-line filtered to 0.1–330 Hz. The head position inside the helmet was continuously monitored using five head position indicator (HPI) coils. The location of each coil relative to the anatomical fiducials (i.e., the nasion, and left and right preauricular points) was defined with a 3D digitizer (FastrakPolhemus, Colchester, VA). Digitalization of the fiducials plus 200 additional points distributed over the participant's scalp were used during subsequent data analysis to spatially align the MEG sensor coordinates to the native T1 high-resolution 3D structural MRI. Structural images were acquired before and 3 months after surgery for each participant with a Siemens 3T MAGNETOM PRISMAfit MR scanner (Siemens, Munich, Germany) in a separate session (i.e., 1 day before the MEG session). T1-weighted MPRAGE anatomical volumes were acquired with the following parameters: echo time = 2.97 ms, repetition time = 2,530 ms, flip angle = 7° and field of view = 256 × 256 × 176 mm^3, number of axial slices = 176, slice thickness = 1 mm, in-plane resolution = 1 mm × 1 mm. The T2-weighted fluid-attenuated inversion recovery (FLAIR) sequence used the following parameters: echo time = 394 ms, repetition time = 5,000 ms, flip angle = 7° and field

TABLE 2 Behavioral results. Mean (M) and SD of accuracy and reaction time (RT) in each condition for each group, with p-values from Welch's t-tests comparing performance between patients and controls and Wilcoxon signed-rank for pre- versus post-surgery stages within the patient's group

	Controls M (SD)	Patients (PRE) M (SD)	Patients (POST) M (SD)	Controls versus patients (PRE) p-value	Controls versus patients (POST) p-value	Patients PRE versus POST p-value
Accuracy (%)						
Object naming	98.75 (2.06)	98.27 (2.83)	98.27 (2.83)	.71	.71	1.0
Action naming	97.5 (3.33)	97.6 (3.63)	95.43 (3.54)	.93	.24	.34
Reaction time (ms)						
Object naming	946.6 (275.5)	963.8 (144.5)	958.8 (219.2)	.36	.74	.68
Action naming	1,059.2 (263.7)	1,105.4 (191.3)	1,096.2 (196)	.36	.44	.68

TABLE 3 Comparison of individual patient scores to control group performance during naming. Mean (M), *t*-values, and *p*-values from Crawford-Howell *t*-tests comparing accuracy and reaction time (RT) during object and action naming before and after surgery for tumor resection

	Pre-surgery			Post-surgery		
	Mean	*t*-value	*p*-value	Mean	*t*-value	*p*-value
Object naming						
Reaction times (ms)						
P1	958.76	0.04	.96	1,014.09	0.23	.81
P2	1,198.29	0.88	.38	1,357.76	1.45	.16
P3	868.91	−0.27	.78	789.25	−0.55	.58
P4	818.81	−0.45	.65	762.78	−0.64	.52
P5	1,067.23	0.42	.67	973.62	0.09	.92
P6	870.76	−0.26	.79	855.33	−0.32	.75
Accuracy (%)						
P1	96.29	−1.16	.26	96.29	−1.16	.26
P2	93.33	−1.21	.24	93.33	−1.21	.24
P3	100	0.58	.56	100	0.58	.56
P4	100	0.58	.56	100	0.58	.56
P5	100	0.58	.56	100	0.58	.56
P6	100	0.58	.56	100	0.58	.56
Action naming						
Reaction times (ms)						
P1	1,004.07	−0.20	.84	1,087.4	0.10	.91
P2	1,444.15	1.42	.17	1,467.46	1.5	.15
P3	890.12	−0.62	.54	882.57	−0.65	.52
P4	1,027.25	−0.11	.9	1,022.13	−0.13	.89
P5	1,177.37	0.43	.67	1,071.77	0.04	.96
P6	1,089.62	0.11	.91	1,046.11	−0.04	.96
Accuracy (%)						
P1	100	0.72	.47	100	0.72	.47
P2	92.6	−1.43	.17	92.6	−1.43	.17
P3	100	0.72	.47	100	0.72	.47
P4	93.33	−1.21	.24	93.33	−1.21	.24
P5	100	0.72	.47	93.33	−1.21	.24
P6	100	0.72	.47	93.33	−1.21	.24

of view = 256 × 256 × 176 mm^3, number of axial slices = 192, 1 mm isotropic resolution.

2.5 | MEG data pre-processing

Continuous data were initially pre-processed off-line using the temporal extension of the signal space separation method (Taulu and Simola, 2006) implemented in Maxfilter 2.2 (Elekta-Neuromag), which subtracts external magnetic noise from the MEG recordings, corrects for head movements and interpolates bad channels with algorithms implemented in the software. Subsequent analyses were performed using the FieldTrip toolbox version 20170911(Oostenveld, Fries,

Maris, & Schoffelen, 2011) in MatlabR2014B. Recordings were downsampled to 500 Hz and segmented into epochs time-locked to stimulus presentation (i.e., picture to be named) from 500 ms before image onset to 1,000 ms after image onset.

Data were filtered with a DFT filter to remove line noise. A semiautomatic procedure was then employed to remove epochs with electromyographic artifacts, SQUID jumps and flat signal. A fast independent component analysis (ICA) was used to identify eye movements, blinks and electrocardiographic artifacts (Jung et al., 2000). The datasets of four healthy participants were excluded from the analysis due to excessive blinking and/or muscular artifacts resulting in the loss of a large number of trials (∼70%). Thus, subsequent analyses were performed on a total of 16 healthy participants.

2.6 | Sensor level analysis

Time-frequency representations (TFR) were calculated from the artifact-free MEG segments for frequencies ranging from 1 to 30 Hz. TRFs were obtained using Hanning tapers and a fixed window length of 500 ms advancing in 10 ms steps, giving rise to a 2 Hz frequency resolution. Power estimates were calculated separately for each orthogonal direction of a gradiometer pair and then combined, resulting in 102 measurement channels. Power was expressed as relative change with respect to a ~500 ms pre-stimulus baseline. On average, conditions comprised 42.33 (SD = 2.02) artifact- and error-free trials for patients (no differences in trial number between object and action naming conditions or pre- and post-surgery sessions, Wilcoxon signed rank, all ps > .11) and 46.22 (SD = 7.22) for healthy controls (no difference between object and action conditions, p = .22). Importantly, no differences in the number of trials between patients and healthy adults were observed for object and action naming either before or after surgery (Welch's t-tests, all ps > .18).

2.7 | Selection of frequency-band and time-windows

Previous M/EEG studies indicate that power changes in the alpha and beta frequency-bands (Piai, Roelofs, Rommers, & Maris, 2015) reflect the retrieval of lexical-semantic information. Furthermore, evidence from studies on stroke (Kielar et al., 2016; Piai et al., 2017; Spironelli et al., 2013) and brain tumor patients (Lizarazu et al., 2020; Traut et al., 2019) points to an involvement of alpha and beta activity in functional compensation. Thus, we focused our analysis on low-frequency activity including alpha (8–12 Hz) and beta (13–28 Hz) oscillations. The time window was primarily chosen based on methodological constraints imposed by our task. Indeed, previous studies show that in overt production tasks artifact-free brain recordings can be measured up to approximately ~400 ms post-stimulus presentation (Ganushchak, Christoffels, & Schiller, 2011). Based on this evidence and visual inspection of the onset of speech production in our data, we focused our TFR analysis to the 0–500 ms time window after picture onset. More specifically, we selected two time-windows capturing early (0–200 ms) and late (200–500 ms) picture-naming related processes, including visual recognition, and conceptualization and lexical selection, respectively (Indefrey, 2011; Indefrey & Levelt, 2004; Liljestrom, Kujala, Stevenson, & Salmelin, 2015).

2.8 | Statistical analysis

In order to evaluate functional compensation within patients' language network we first explored the spectro-temporal pattern of responses triggered by our picture naming task in a group of healthy controls. More specifically, we calculated TFRs for object and action naming in early and late time-windows relative to picture onset and compared each of them relative to pre-stimulus baseline activity.

Then, once main oscillatory patterns triggered by the task were identified in controls, we assessed longitudinal changes in the group of patients. Specifically, we calculated TFRs for object and action naming before tumor resection and contrasted them with those obtained 3 months after the surgery.

In all cases, differences in spectral power between conditions at the sensor level were assessed using cluster-based permutation tests (Maris & Oostenveld, 2007). This test controls for multiple comparisons using a cluster-based correction while maintaining sensitivity based on temporal, spatial and frequency dependency of neighboring samples. The permutation p-value was calculated using the Monte Carlo method with 1,000 random permutations. The threshold for significance testing was a p-value below 5% (two-tailed). Please note that the finding of a significant cluster implies that there is a significant difference between conditions. However, the cluster does not provide exact information about the timing and the spatial location of the effect. In other words, no statements about the onset/offset of the effect at the millisecond level or about its spatial extent can be made (Sassenhagen & Draschkow, 2019). While we had clear hypotheses about the frequency-bands potentially involved in the language effects (i.e., alpha-beta), no specific a priori hypotheses about timing and/or location were held. Thus, we averaged over frequency bins (alpha central frequency = 10.13 Hz and beta central frequency = 20.66 Hz;) but considered all sensors (i.e., combined gradiometers) and time-points within early and late time-windows in the analysis.

2.9 | Source localization

Participants' high-resolution 3D structural MRIs were segmented using Freesurfer software (Dale & Sereno, 1993). Co-registration between the MEG sensor coordinates and the participant's MRI coordinates was done by manually aligning the digitized head-surface and fiducial points to the outer scalp surface. The forward model was computed using the Boundary Element Method (BEM) implemented in the MNE software suite (Gramfort et al., 2014); RRID:SCR_005972) for three orthogonal tangential current dipoles (one for each spatial dimension) placed on a homogeneous 5-mm grid source space covering the whole brain. For each source, the forward model was then reduced to its two principal components of highest singular value, which closely correspond to sources tangential to the skull. We used both gradiometers and magnetometers in the source estimation, normalizing each sensor signal by its noise variance (500-ms baseline period prior to picture onset). Brain source activity was calculated for each participant using Linearly Constrained Minimum Variance (LCMV) beamformer approach (Van Veen, van Drongelen, Yuchtman, & Suzuki, 1997). A common filter was computed by combining the cross-spectral density (CSD) matrices from the time-frequency window of the significant sensor-level effects and an equally-sized baseline period prior to picture onset. The common filter was then applied separately to each condition to estimate source power. Since we focused our analysis on the local source power, we

only used real-valued filter coefficients (Grutzner et al., 2010). To normalize source activity, the neural activity index (NAI) was calculated as a certain ratio between the power in the experimental conditions and the pre-stimulus baseline (Pcond-Pbase./Pbase). For each session (pre- and post-surgery), the MEG maps were first co-registered with their corresponding individual MRIs and then normalized to the standard MNI to run group level analyses. This was done by applying a non-linear transformation using the spatial-normalization algorithm implemented in SPM8 and it was checked by one of the authors (LA).

Group analyses were performed with the location-comparison method described in (Bourguignon, Molinaro, & Wens, 2018). Briefly, this method generates bootstrap group-averaged maps to build a permutation distribution of location difference between local maxima in the two conditions being compared, and test the null hypothesis that this distance is zero. Local maxima is defined as sets of contiguous voxels displaying higher power than all other neighboring voxels. The threshold for statistical testing at $p < .05$ was computed as the 95-percentile of the permutation distribution. All supra-threshold local MEG peaks were interpreted as indicative of brain regions likely triggering the sensor-level effects. This robust method has shown to deal well with the spectral leakage of the source-projected MEG data which can result from directly contrasting brain maps for different conditions.

2.10 | 3D lesion reconstruction

Lesions were manually drawn on the native space of participants' T1-weighted MPRAGE image by a trained technician using the MRIcron software (Rorden, Karnath, & Bonilha, 2007) and further supervised by the neurosurgeons in charge of the patients' awake craniotomy (SGR and IPG). The reconstruction was performed also using information from T2 images when lesion boundaries were not clear in the T1 MRI. The lesion was then normalized to the MNI template and alignment between the reconstructed lesion and the lesion in the native space was checked by one of the authors (IQ). A volume of interest (VOI) was created for each patient each time point. From each pre- and post-surgery 3D reconstruction, the tumor volume (cm^3) was calculated. Extent of resection (cm^3) was measured on postoperative imaging as: (Volume of (preoperative 3D Tumor Reconstruction ∩ postoperative Resection)*100/preoperative tumor volume).

2.11 | Structural measure of white mater changes

For the structural analysis, preoperative and postoperative T1 and T2 images were pre-processed and analyzed using the Voxel-Based Morphometry (VBM) toolbox and the SPM12 software package. Images were corrected for bias-field inhomogeneity; classified into gray, white matter and cerebrospinal fluid; registered to a standard MNI space using high-dimensional DARTEL normalization (Ashburner, 2007) and further smoothed with a 6 mm full width half maximum (FWHM) Gaussian kernel. We used a segmentation approach based on an adaptive maximum,

a posterior technique which does not need a priori information about tissue probabilities (Rajapakse, Giedd, & Rapoport, 1997). We further refined this procedure, by accounting for partial volume effects and by applying a hidden Markov random field model which incorporates spatial prior information of the adjacent voxels into the segmentation estimation (Tohka, Zijdenbos, & Evans, 2004).

To assess potential differences in white matter involvement we used a region of interest (ROI) approach. ROIs were defined using a probabilistic tractography atlas (Rojkova et al., 2016). The selected tracts were the superior longitudinal fasciculus (SLF I), the arcuate fasciculus (AF, long branch) and the inferior-fronto-occipital fasciculus (IFOF), which constitute key bundles within dorsal and ventral language pathways and their damage is known to affect language processing (Agosta et al., 2013; Almairac, Herbet, Moritz-Gasser, de Champfleur, & Duffau, 2015; Catani & Mesulam, 2008; Mandelli et al., 2014). For each of these ROIs, we extracted preoperative and postoperative mean volumes in left and right hemispheres and corrected it for brain size using the total intracranial volume (TIV). By doing so, we obtained a proxy marker of white matter involvement based on lesion distribution in relation to white-matter probabilistic distribution derived from the tractography atlas (Rojkova et al., 2016). Comparisons between patient's morphometric values and controls were performed using Crawford-Howell t-tests.

2.12 | Correlational analysis between structure and function

First, we calculated a Language laterality index (LI) using the following formula:

$$LI = (R - L)/(R + L).$$

where "R" and "L" represent power averaged across sensors for naming conditions (object and action pooled together) in right and left hemispheres, respectively; thus yielding positive values for right-lateralized and negative values for left-lateralized language-related activity. Given the left-lateralized pattern of oscillatory beta responses observed in the healthy control group as well as previous studies using beta power for calculating LI in speech production tasks (Traut et al., 2019), we reasoned that beta activity (13–28 Hz) was better suited than alpha to capture a potential shift toward the right hemisphere triggered by tumor presence and/or resection. Thus, the index was calculated for each patient and session (i.e., before and after surgery) only in the beta band. Furthermore, given the common left-lateralized pattern observed in both object and action naming, we combined them into a unique naming condition to reduce dimensionality and obtain a higher signal-to-noise ratio in the data. Please note, that this methodological choice (i.e., focus on beta responses) was further supported by the longitudinal contrast in patients, showing oscillatory effects circumscribed to the beta frequency-band (see below). LI was tested separately in controls and patients with Wilcoxon signed rank tests against zero and between groups using Welch's t-tests.

In addition, the same index was used to calculate lateralization of white matter tracts in controls and patients. More specifically, in the case of patients, this index was calculated separately in preoperative and postoperative stages and, in each case, individually compared against the control group using Crawford-Howell *t*-tests.

Finally, Pearson correlations between preoperative and postoperative white matter ROIs LI and beta longitudinal changes (post − pre-surgery beta LI) were run to establish whether potential reshaping at the structural level was associated with functional one.

3 | RESULTS

3.1 | Behavioral results

Table 2 shows mean accuracy and reaction time values (RT) for healthy controls and patients, as well as contrasts between groups and surgery stages. Overall, no differences in performance (i.e., accuracy and RTs) were observed between groups. These results were further confirmed at the individual patient level with Crawford-Howell *t*-tests, which supported the absence of significant behavioral effects (see Table 3). In addition, no differences were observed within patients when comparing performance before and after surgery. This finding was well expected, given that patients with slow-growing

brain tumors typically exhibit a normal neurological and behavioral exploration, at least when considering relatively easy low-level tasks (DeAngelis, 2001). Furthermore, the maintenance of this behavioral pattern after surgery speaks in favor of successful language compensation.

3.2 | Oscillatory signatures of picture naming in healthy controls

Figure 2 shows the time-frequency representations (TFRs), topographical distributions and source localization plots of the naming conditions as compared to baseline in the alpha (8–12 Hz) and beta (13–28 Hz) frequency-bands.

Early time-window effects (0–200 ms): Object and action naming showed early alpha power increases as compared to baseline. This effect was highlighted by significant positive clusters (both Monte Carlo *p*s = .004, two-tailed), over bilateral posterior and left middle sensors, in the case of objects; and bilateral posterior sensors in the case of actions. Source localization of early alpha effects identified the related local maxima in occipito-parietal regions. In addition, similar beta power increases were observed for object and action naming conditions as indicated by significant positive clusters over left posterior and middle sensors (both Monte Carlo *p*s = .01, two-tailed).
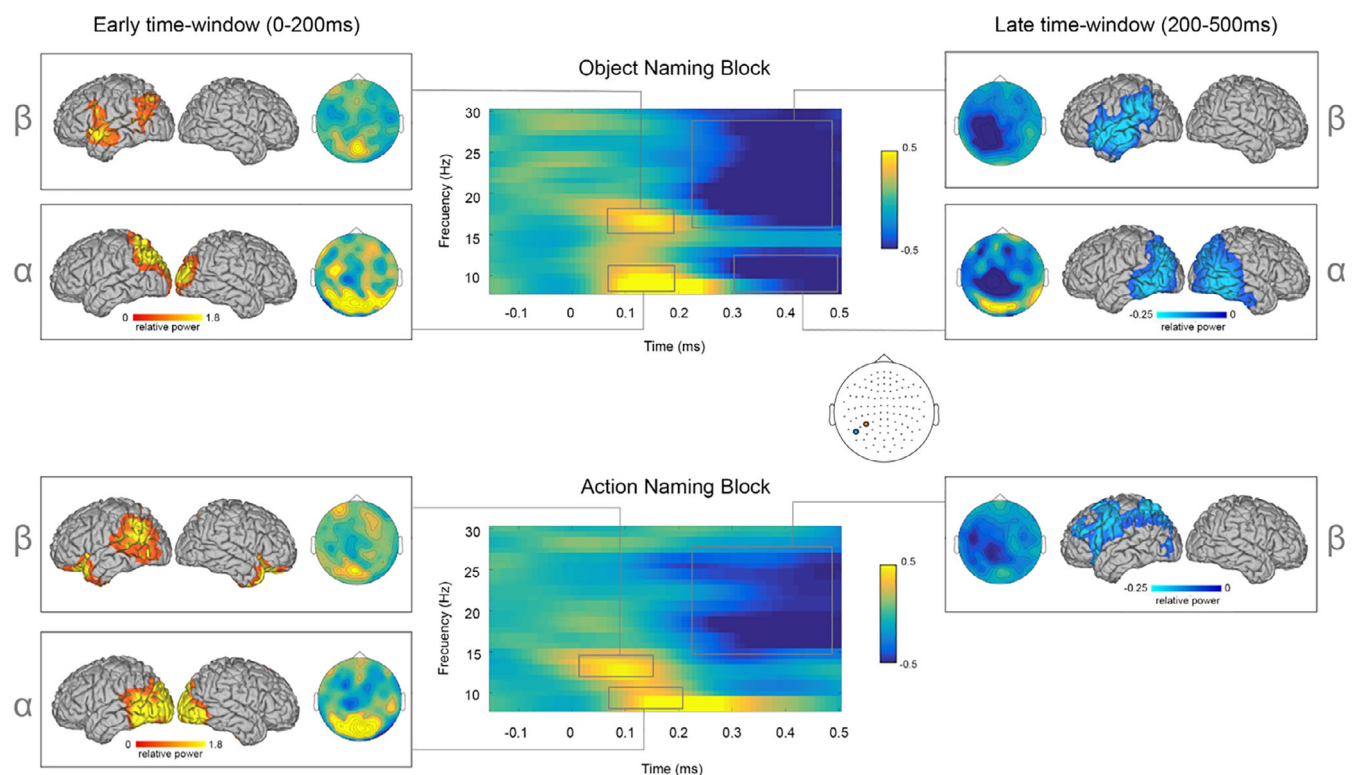

FIGURE 2 Oscillatory signatures of speech production in healthy controls. TFR of alpha and beta power in the object (top panel) and action (bottom panel) conditions over time. TFRs are plotted as relative power change compared to the baseline period over representative significant sensors (objects = M1632 + M1633; highlighted in orange; actions = M1722 + M1723; highlighted in blue). Topographic distribution plots show posterior alpha and beta power increases at early stages (0–200 ms), and left-lateralized anterior and posterior beta power decreases at later stages (200–500 ms)

Source localization showed local maxima peaking in left angular gyrus and inferior frontal gyrus (IFG) for objects; and in left supramarginal and orbitofrontal areas for actions (Figure 2, right panel).

Late time-window effects (200–500 ms): During this period, a significant negative cluster (Monte Carlo *p* = .01, two-tailed) encompassing bilateral posterior and middle sensors revealed alpha power decreases only for the object naming condition. At the source level, this effect showed local minima in bilateral occipito-temporal regions.

Finally, both conditions showed beta power decreases that were underscored by significant negative clusters over bilateral posterior and anterior sensors in the case of objects (Monte Carlo *p* = .004, two-tailed); and bilateral posterior and left anterior sensors in the case of actions (Monte Carlo *p* = .01, two-tailed). Source localization of beta effects showed local minima in the left IFG, irrespectively of the naming condition, while object naming additionally recruited the left anterior temporal pole and action naming the left superior parietal and dorsal premotor cortex (Figure 2, left panel).

Overall, these findings provide a baseline to interpret potential language reshaping in patients. In brief, they support previous M/EEG studies (Piai et al., 2015, 2017) showing the involvement of alpha-beta oscillations in speech production and align well with evidence indicating the existence of partially non-overlapping networks for the processing of object and action knowledge, showing a diverse contribution of ventral and dorsal nodes of the language network, respectively (Vigliocco et al., 2011).

3.3 | Functional plasticity in brain tumor patients

Figure 3 shows TFRs, topographic distributions of the object effect found in patients with ventral temporal lesions (Figure 3a) and of the action effect, found in patients with dorsal fronto-parietal lesions (Figure 3b). Overall, when comparing oscillatory activity across sessions (post- vs. pre-surgery for tumor resection) within each group of patients, we found significant differences between sessions in the beta band (13–28 Hz), with power increases after tumor resection.
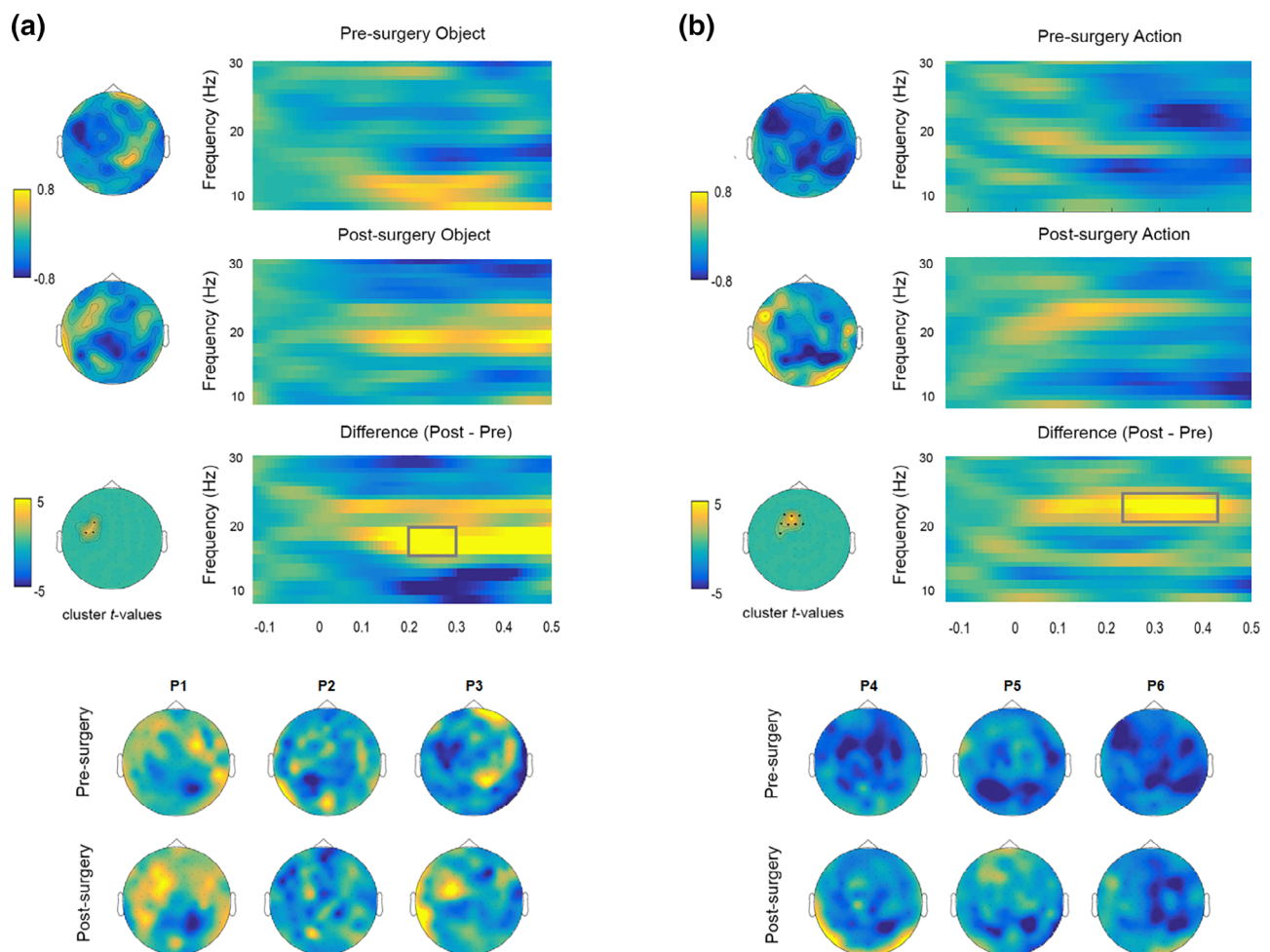

FIGURE 3 Longitudinal functional plasticity in brain tumor patients. (a) TFRs of patients with ventral lesions showing beta power increases after surgery only for objects; (b) TFRs of patients with dorsal lesions showing a similar effect but only for actions. TFRs are plotted as relative power changes compared to the baseline period in averaged significant sensors (shown in black over the topographical distribution of the significant clusters)

Longitudinal effect for objects in patients with ventral lesions. A positive cluster (Monte Carlo *p* < .001, two-tailed) over left frontal sensors highlighted the presence of significant differences between pre and post conditions in the beta range. No effects were observed in the alpha range (all *p*-clusters > .24). Importantly, no significant differences were observed for the action naming condition in any of the low-frequency bands (all *p*-clusters > .46). Source localization of the object-related beta effect involved the left IFG and the right posterior middle temporal cortex (see Figure 4).

Longitudinal effect for actions in patients with dorsal lesions. A positive cluster was found over left frontal sensors (Monte Carlo *p* = .001, two-tailed), underscoring post vs. pre significant differences in the beta range. No effects were found in alpha activity (all *p*-clusters > .49). Importantly, no differences were observed for the object condition in any of the low-frequency bands (all *p*-clusters > .25). Source localization of the action-related beta effect involved the left IFG, the right middle-frontal gyrus, the right superior parietal and the right dorsal premotor cortex (see Figure 4).

3.4 | Structural reshaping in patients

To detect possible alterations in right white matter structures as a consequence of left-hemispheric tumor growth (i.e., preoperative) and /or neurosurgical intervention (i.e., postoperative), we estimated a proxy measure of white matter volume in language-related tracts of interest in patients and healthy controls. First, we measured ROI volumes in patients and controls within each hemisphere and compared them separately using Crawford-Howell *t*-tests. This was done to rule out that potential differences in LI were trivially quantifying the damage in the left hemisphere rather than compensatory volume increases. Table 4 shows patients mean TIV-normalized preoperative and postoperative volume values for each white matter ROI in each hemisphere as well as comparison statistics at the individual level. When comparing TIV-normalized values in left and right ROI before surgery, differences between patients and controls were observed in all the tracts irrespectively of the hemisphere (all *ps* < .001). After
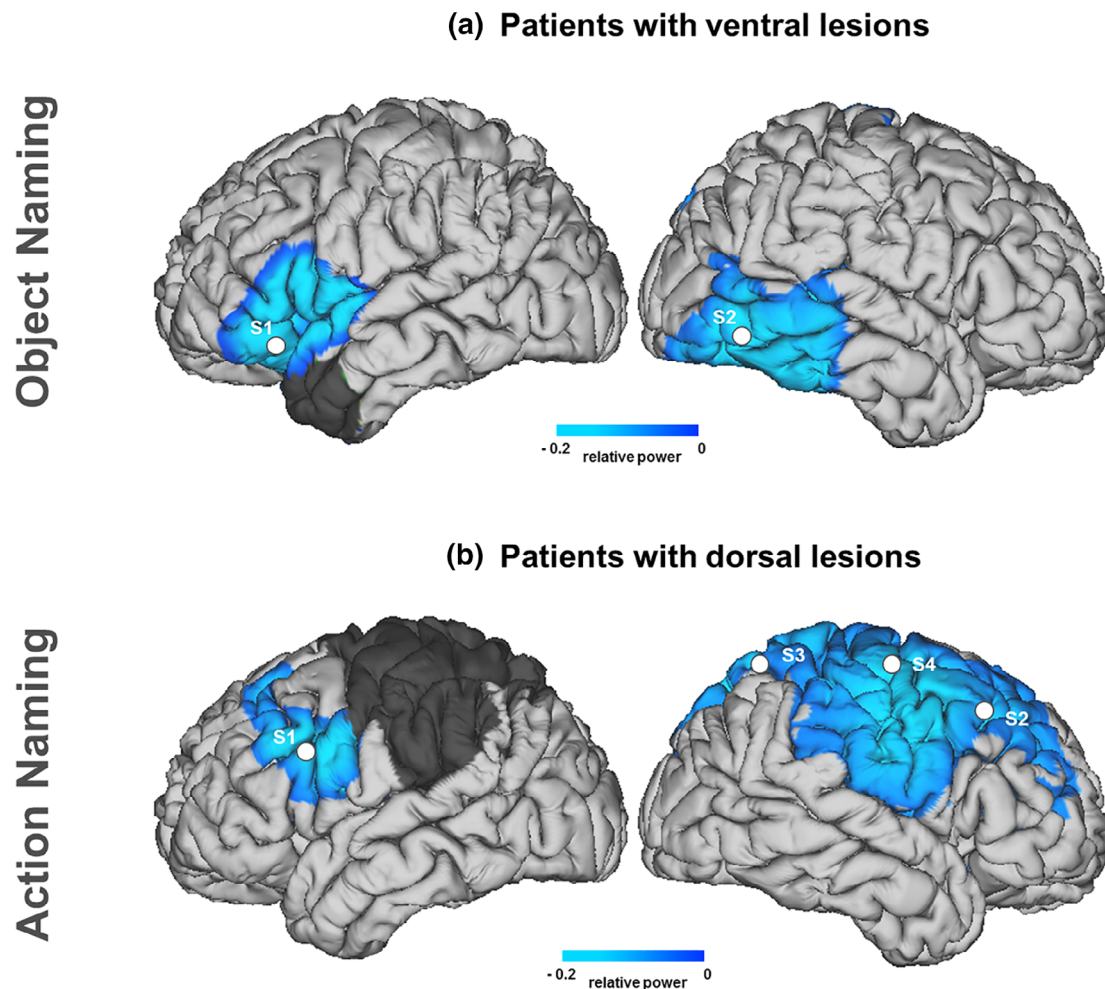

FIGURE 4 Source reconstruction of oscillatory longitudinal effects (post vs. pre). Regions showing beta power changes for patients with ventral (a) and dorsal (b) lesions. Significant peak activity locations (MNI coordinates [*x, y, z*]) within these areas are marked with white dots. Post-surgery lesion mask overlap is displayed in gray. For the object naming condition: S1 = left IFG [BA45: −52, 19, 4] and S2 = right posterior middle-temporal gyrus [BA21: 64, −36, −1]. For the action naming condition: S1 = left IFG [BA44: −50, 16, 27], S2 = right medial-frontal gyrus [BA9: 34, 39, 34], S3 = right superior parietal cortex [BA7: 19, −67, 62], and S4 = right dorsal premotor cortex [BA6: 43, −7, 50]

surgery, most of the patients showed no differences with controls in any of the ROI. However, patient 6 showed differences in the left AF and left SFL, and patient 4 in the left SLF.

Afterwards, we calculated ROI laterality indexes in patients (before and after surgery) and controls and used Crawford-Howell t-tests to compare each patient against the control group (see Table 5). Before surgery, all patients showed significant alterations in ROI lateralization as compared to controls in the AF and the IFOF. Also, most of them showed differences in the SLF with the exception of patients 2 and 5. After the surgery, no differences between controls and patients were observed for IFOF lateralization. Similarly, in the case of the AF, most of the patients showed no differences when compared to controls, with the exception of patient 6 and 3. Finally, in the case of the SLF, the patients with ventral damage showed no differences with controls. However, those patients with dorsal lesions, showed a significant shift in ROI lateralization toward the right, contralesional hemisphere.

3.5 | Correlational analysis between functional and structural laterality indexes

In healthy controls, a Wilcoxon signed rank test against zero showed that beta power was lateralized toward the left hemisphere ($W = 102$, $p = .04$, $M = -0.22$, $SE = 0.13$). The same test performed in patients showed a leftward lateralization of language-related beta activity before surgery ($W = 21$, $p = .03$, $M = -0.13$, $SE = 0.04$) and a rightward shift after tumor resection ($p = .03$, $M = 0.61$, $SE = 0.24$; see Figure 5a). When comparing patients to controls, no significant differences were observed before tumor resection (Welch $t[17] = -0.65$, $p = .51$; Cohen's $d = -0.24$). However, after surgery, patients significantly differed from controls ($t[8] = 3.05$, $p = .01$; Cohen's $d = 1.5$), with this effect likely reflecting the shift of beta power toward the right hemisphere. See Figure 5a.

Finally, we correlated structural ROI LIs with the beta longitudinal LI and found a significant positive correlation between beta and post-surgery SLF laterality index (Pearson $r = 0.92$; $p = .009$), overall indicating that postoperative lateralization of beta power and SLF toward the right hemisphere were associated (see Figure 5b).

4 | DISCUSSION

In the present study, we considered brain tumor patients as an experimental model to test oscillatory patterns supporting language plasticity and reorganization. Specifically, we combined functional and structural measures by means of MEG and MRI and: (a) tracked the oscillatory dynamics subserving object and action naming in the intact and the damaged brain; (b) measured structural reshaping in contralesional white matter tracts involved in language processing. Overall, two main findings can be underscored. First, longitudinal functional changes in object and action naming within patients were observed in the beta band. Interestingly, plasticity patterns were specifically

TABLE 4 Volume values of white matter ROIs in patients and comparison statistics. Individual patients TIV-normalized volumes for white matter regions of interest (ROI) before (PRE) and after (POST) surgery within each hemisphere, including the superior longitudinal fasciculus (SLF), arcuate fasciculus (AF) and inferior fronto-occipital fasciculus (IFOF). Crawford-Howell t-values and p-values comparing each patient to the control group are provided

	PRE	t-value	p-value	POST	t-value	p-value
SLF left						
P1	0.0926	13.6	<.001	0.0411	1.13	.27
P2	0.102	15.8	<.001	0.0424	1.34	.19
P3	0.0862	12	<.001	0.0377	0.3	.76
P4	0.0938	13.8	<.001	0.024	−3	.008
P5	0.0903	13	<.001	0.024	−3	.008
P6	0.101	15.6	<.001	0.0302	−1.5	.15
SLF right						
P1	0.085	12.3	<.001	0.039	1.06	.3
P2	0.095	14.8	<.001	0.039	1.06	.3
P3	0.077	10.4	<.001	0.036	0.33	.74
P4	0.0844	12.2	<.001	0.036	0.33	.74
P5	0.0839	12	<.001	0.0344	−0.06	.95
P6	0.0897	13.5	<.001	0.0356	0.23	.81
AF left						
P1	0.0534	12.5	<.001	0.0219	−1.09	.29
P2	0.0582	14.5	<.001	0.0229	−1.04	.31
P3	0.0498	10.9	<.001	0.0237	−0.31	.76
P4	0.0542	12.8	<.001	0.0225	−0.82	.42
P5	0.0517	11.7	<.001	0.021	−1.47	.16
P6	0.0585	14.7	<.001	0.0148	−4.14	<.001
AF right						
P1	0.0356	4.79	<.001	0.022	−0.53	.6
P2	0.0391	6.43	<.001	0.022	−0.53	.6
P3	0.0335	3.98	<.001	0.02	−1.35	.19
P4	0.0349	4.79	<.001	0.02	−1.35	.19
P5	0.035	4.79	<.001	0.021	−0.93	.36
P6	0.0389	6.02	<.001	0.021	−0.93	.36
IFOF left						
P1	0.092	11.5	<.001	0.036	0.17	.86
P2	0.101	−5.08	<.001	0.035	0.049	.96
P3	0.0838	9.86	<.001	0.036	0.17	.86
P4	0.0913	11.4	<.001	0.0355	−0.03	.97
P5	0.0891	10.9	<.001	0.0357	0.11	.91
P6	0.0982	12.8	<.001	0.0345	−0.13	.89
IFOF right						
P1	0.088	10.2	<.001	0.0387	0.44	.66
P2	0.096	11.8	<.001	0.0394	0.58	.56
P3	0.08	8.65	<.001	0.0385	0.41	.68
P4	0.087	10	<.001	0.0377	0.25	.8
P5	0.086	9.84	<.001	0.0383	0.37	.7
P6	0.092	11	<.001	0.0374	0.19	.85

	LI pre	t-value	p-value	LI post	t-value	p-value	% LD
SLF I							
Controls	−0.0254						
P1	−0.043	−2.22	.04	−0.023	0.28	.78	0
P2	−0.039	−1.72	.1	−0.039	−1.72	.1	0
P3	−0.054	−3.6	.002	−0.015	1.28	.21	0
P4	−0.052	−3.35	.004	0.191	26.9	<.001	0.338
P5	−0.036	−1.34	.19	0.178	25.4	<.001	15.358
P6	−0.06	−4.35	<.001	0.082	13.4	<.001	3.676
AF							
Controls	−0.0243						
P1	−0.199	−13.6	<.001	0.002	2.03	.06	0
P2	−0.195	−13.3	<.001	−0.012	0.93	.36	0
P3	−0.195	−13.3	<.001	−0.072	−3.74	.001	0.016
P4	−0.215	−14.9	<.001	−0.042	−1.4	.18	0
P5	−0.192	−13.1	<.001	−0.0002	1.85	.08	0.767
P6	−0.201	−13.8	<.001	0.174	15.4	<.001	3.941
IFOF							
Controls	0.0186						
P1	−0.022	−3.12	.007	0.028	0.73	.47	0.03
P2	−0.026	−3.43	.003	0.053	2.66	.01	0
P3	−0.018	−2.81	.01	0.032	1.04	.31	0
P4	−0.023	−3.19	.006	0.029	0.81	.43	0
P5	−0.012	−2.35	.03	0.034	1.2	.25	0
P6	−0.028	−3.58	.002	0.039	1.58	.13	0.554

TABLE 5 Comparison of individual patient white matter ROI lateralization index to control group profiles. Laterality indexes (LI), t-values and p-values from Crawford-Howell t-tests comparing preoperative and postoperative lateralization profiles of white matter ROIs in each individual patient against the control group. Percentage (%) of damage to the tract in the left hemisphere is provided
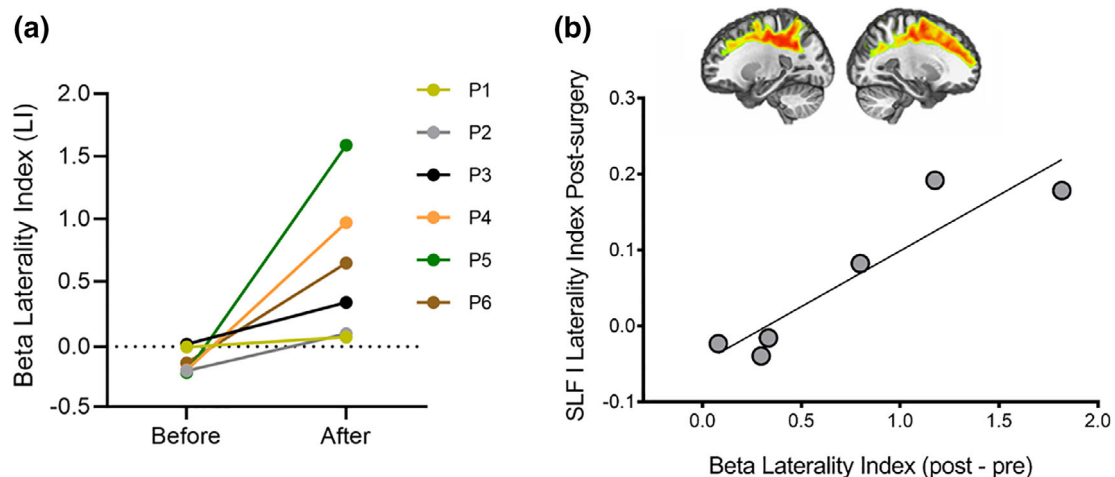

FIGURE 5 Structural reshaping and association with beta power lateralization. (a) Beta laterality index (LI) before and after tumor resection is shown for each individual patient. Positive values indicate rightward lateralization, negative values indicate leftward laterlization. (b) Scatterplot shows significant positive correlation between SLF lateralization after surgery and beta longitudinal LI (post − pre-surgery LI)

related to tumor location, with ventral damage leading to compensation in object naming and dorsal damage to compensation in action naming. Of note, this category-related dissociation was present in healthy controls, with beta power decreases showing a different engagement of ventral and dorsal nodes in the language network during object and action naming, respectively (Gleichgerrcht et al., 2016; Lubrano et al., 2014; Vigliocco et al., 2011). Second, at the structural level, patients showed preoperative reshaping in white matter regions underscored by significant lateralization differences in the IFOF, the AF and the SLF as compared to controls. Postoperative

differences were also evident mostly in patients with dorsal damage, showing a rightward shift in SLF lateralization. Interestingly, this structural change positively correlated with the longitudinal shift of beta power toward the right hemisphere, suggesting that functional and structural components of brain plasticity go hand to hand in language reorganization.

Oscillatory signatures of speech production in the intact brain. We first ran a picture-naming task in a group of healthy participants in order collect normative data to better understand the potential uniqueness of patients' responses due to language reshaping. When considering previous studies measuring speech production in healthy adults, beta activity has been classically associated to motor aspects involved in articulation (Saarinen, Laaksonen, Parviainen, & Salmelin, 2006; Salmelin & Sams, 2002). However, as precisely pointed out by Piai et al. (2015) these studies compared the production of words vs. pseudo-words, which do not exist in memory and hence do not allow tapping into memory and semantic components involved in speech production. Here, by using a picture-naming task— which does capture the aforementioned aspects—we found a left involvement of beta activity which, in keeping with previous findings (Laaksonen, Kujala, Hulten, Liljestrom, & Salmelin, 2012; Liljestrom et al., 2015; Piai et al., 2015), likely reflects lexico-semantic processing of object and action knowledge. Furthermore, beta activity was differently distributed for object and action naming, with the former condition mostly engaging ventro-temporal areas and the latter one parietal and pre-motor regions. In addition, bilateral alpha activity was only observed for object naming. A potential interpretation of these findings is that object and action concepts differed in terms of feature types, with visual features more represented in the object domain and motoric features in the action one (Huttenlocher & Lui, 1979; Vinson, Vigliocco, Cappa, & Siri, 2003). Indeed, this view predicts that, at a neural level, the lexical retrieval of object nouns will mainly recruit occipito-temporal regions storing visual features, while the retrieval of action verbs will mainly recruit motor/pre-motor structures associated to motoric features (Gainotti, Silveri, Daniele, & Giustolisi, 1995; Moseley, Pulvermuller, & Shtyrov, 2013; Pulvermuller, Lutzenberger, & Preissl, 1999). In support of this prediction, object naming showed alpha-beta cortical activations in occipito-temporal areas, while action naming engaged the classical dorsal fronto-parietal network involved in processing action concepts with this effect being mainly circumscribed to beta activity (Kemmerer, Rudrauf, Manzel, & Tranel, 2012; Watson, Cardillo, Ianni, & Chatterjee, 2013).

Nevertheless, due to the overt nature of the task implemented here, it can be argued that beta modulations sourced in the premotor cortex, could actually reflect myogenic activity rather than semantic processing. While we cannot completely rule out this possibility, we find it quite unlikely due to several reasons. First, beta activity preceded vocal responses for more than 400 ms. Second, the beamformer technique used in the present study is known to attenuate myogenic artifacts by suppressing signals whose spatial scalp distribution cannot be explained by a dipolar source in the brain (Piai et al., 2015). Finally, the specificity of the observed effect (i.e., present in the action but not in the object naming condition) speaks in favor

of a category related modulation and fits well with evidence showing that motor beta oscillations sourced in premotor regions play a key role in action semantics (Grisoni, Dreyer, & Pulvermuller, 2016; Hauk, Johnsrude, & Pulvermuller, 2004; Weiss & Mueller, 2012).

4.1 | Neuroplasticity of language in brain tumor patients

Previous studies indicate that patients with slow-growing brain tumors exhibit normal clinical exams -at least when considering standard neuropsychological assessment (Duffau & Capelle, 2001; Walker & Kaye, 2003). In agreement with this evidence, we found that patients were able to correctly retrieve object and action knowledge either before or after surgery, overall suggesting successful reorganization and language preservation.

At the neurophysiological level, when comparing functional patterns longitudinally (post- vs. pre-surgery activity), beta rhythms (13–28 Hz) were called into play. Beta synchronization is assumed to facilitate long-range communication between distant brain areas supporting high-level interactions (Kopell, Ermentrout, Whittington, & Traub, 2000; Varela, Lachaux, Rodriguez, & Martinerie, 2001). Furthermore, it has been shown that increased beta connectivity between distant brain regions correlates with greater quality of life in brain injured patients (Castellanos et al., 2010). Thus, this brain rhythm may play a key role in the successful recruitment of remote ipsilesional and contralesional regions necessary to preserve high-level cognitive functions at the network level. Interestingly, beta power modulations varied depending on damage location and semantic category, with ventral and dorsal lesions specifically modulating object and action naming, respectively. These findings align well with the dissociation observed in the group of healthy controls and with previous evidence (Gleichgerrcht et al., 2016; Kemmerer et al., 2012; Pisoni et al., 2018; Tranel, Adolphs, Damasio, & Damasio, 2001; Vigliocco et al., 2011) suggesting a differential engagement of temporal and fronto-parietal regions in object and action naming. Nevertheless, our results contrast with the dominant view suggesting that frontal areas are exclusively associated to action processing. Indeed, we found evidence for increased beta activity in the left IFG irrespectively of the naming condition, possibly reflecting controlled semantic retrieval (Noonan, Jefferies, Visser, & Lambon Ralph, 2013) or lexical selection processes (Thompson-Schill, D'Esposito, & Kan, 1999).

When considering the net output of the longitudinal analysis, patients with ventral and dorsal lesions showed overall increases in beta power after tumor resection. However, while in the dorsal group power decreases were present both before and after surgery, being larger before tumor resection; in the ventral group, power increases were present after but not before surgery. Thus, even though the net output is similar (i.e., beta power increases), these effects might involve distinct physiological mechanisms. In the first case, less power decreases after tumor resection seem to reflect, as shown by their topographical distribution, a downregulation of left frontal activity, which was instead playing a stronger role before tumor resection,

possibly through the compensatory recruitment of ipsilesional frontal areas as it has been previously shown in the literature (see Spironelli et al., 2013). In the second case, left frontal beta power decreases present in the preoperative but absent in the postoperative stage, likely indicate the disengagement of left frontal nodes following tumor resection. Nevertheless, these assumptions are rather speculative and further studies need to zoom into the different compensatory mechanisms and their relation to tumor resection.

From an anatomical standpoint, longitudinal beta modulations in patients with ventral damage were localized in the left IFG and the right posterior MTG. These regions have been implicated in the semantic control network (Noonan et al., 2013; Wright, Stamatakis, & Tyler, 2012) and were recruited by controls during object naming, thus likely reflecting compensatory activity in preserved healthy regions. When considering patients with dorsal damage, longitudinal beta power modulations were observed in the left IFG and contralesional healthy homologs, including right superior parietal, premotor and middle-frontal areas. Of note, this latter collection of right areas was not found to be activated in healthy controls during action naming, which instead showed a completely left-lateralized network. Thus, this pattern possibly reflects language reorganization supported by the unmasking of a homolog network in the healthy hemisphere. Indeed, recent studies (Duffau, 2008; Vassal et al., 2010) using direct electrical stimulation have revealed a right mirror organization of language networks, pointing to the existence of functional redundancies that can undertake functions previously supported by damaged areas. Furthermore, this finding also aligns well with neurophysiological evidence from brain tumor (Piai et al., 2020; Traut et al., 2019) and stroke patients (Kielar et al., 2016; Piai et al., 2017) showing compensatory recruitment of the right hemisphere during language processing. Of note, one of these studies (Piai et al., 2017) showed that contralesional recruitment in the alpha-beta band was associated with the integrity of the posterior bundles of the corpus callosum. Indeed, it has been shown that the integrity of these withe matter bundles are critical for recruiting healthy areas contralateral to the lesion (Celeghin et al., 2017).

Here, irrespectively of tumor location, all patients showed preoperative structural reshaping in the SLF connecting parietal and premotor cortex (Kamali, Flanders, Brody, Hunter, & Hasan, 2014; Makris et al., 2005) the AF (long branch) connecting Broca and Wernicke areas and the IFOF, connecting occipital and frontal regions (Herbet, Moritz-Gasser, & Duffau, 2017). It is well documented that glioma invasions trigger reorganizations at the whole-brain network level which are not circumscribed to the area invaded by the tumor (Cargnelutti, Ius, Skrap, & Tomasino, 2020).

On the one hand, the IFOF has been previously associated with semantic processing (Herbet et al., 2017). The AF and the SLF, on the other hand, have been related to phonological processing and lexical retrieval during language production, since their disruption with DES produces phonological paraphasias and pure anomia, respectively (Sarubbo et al., 2015). While current data do not allow dissociating which of these functions were specifically compensated in the patients, the finding of a positive association between postoperative

right volumetric increases in the SLF and greater beta power in the right hemisphere may suggest that lexical retrieval components were those mostly implicated.

In line with recent studies (Almairac, Duffau, & Herbet, 2018; Zhang et al., 2018) using a VBM approach and showing volumetric increases in contralesional gray matter homologs, here we observed a similar pattern but for white matter ones. Interestingly, Zhang and collaborators (2018) also reported that structural changes correlated with functional ones, such that increased functional activity was related to structural alterations reflected in greater volume, whereas decreased neural activity was independent of structural change. Overall, the authors related macrostructural variations to functional compensation (i.e., suggesting a structure–function coupled response to deal with the tumor), an interpretation that aligns well with our results. However, these studies only analyzed preoperative data. Here, we provide preliminary evidence suggesting not only that similar compensatory mechanisms might be also involved in white matter macrostructural reshaping but that these changes can be observed before but also after surgery.

Nevertheless, it is worth mentioning that the present study is not without limitations. Even though collecting longitudinal data in this type of populations is quite challenging, the most evident limitation is the use of a relatively small sample size, thus requiring caution when generalizing and interpreting current results. Second, we cannot completely rule out the potential effect that differences in corticospinal fluid (CSF) may have in the observed effects. Indeed, one can expect an asymmetrical amount of CSF given that, between the two sessions, resections occurred in only one hemisphere. However, magnetic fields are quite insensitive to CSF conductivity as it has been shown by previous studies (Vorwerk et al., 2014), thus turning unlikely a significant contribution of CSF to the source reconstruction. Nevertheless, future studies are necessary to replicate current findings in larger patient samples and disentangle if observed compensatory patterns can be generalized to a larger population and further specify under which circumstances white matter changes are prone to take place.

5 | CONCLUSIONS

In line with previous neurophysiological findings, our results point to a fundamental role of beta oscillations in language reorganization. Furthermore, by showing white matter changes and their link to the rightward shift in beta laterality following tumor resection, they suggest that structure and function work concertedly in supporting plastic changes involved in this process. Together, these results provide new insights into the potential for language plasticity in preoperative and postoperative stages, which ultimately help to delineate personalized surgical strategies to preserve linguistic functions in brain tumor patients.

through BCBL Severo Ochoa excellence accreditation SEV-2015-0490, by the Ikerbasque Foundation, by a Juan de la Cierva Fellowship to LA (IJCI-2017-31373) and by the Plan Nacional RTI2018-096216-A-I00 (MEGLIOMA) to LA and RTI2018-093547-B-I00 (LangConn) to MC and IQ both funded by the Spanish Ministry of Economy and Competitiveness. The authors would like to thank all the patients who took part in this study.

CONFLICT OF INTEREST
The authors declare no potential conflict of interest.

DATA AVAILABILITY STATEMENT
Data availability statement: The data that support the findings of this study are available from the corresponding author upon reasonable request.

ORCID
Lucia Amoruso https://orcid.org/0000-0003-4696-2187

REFERENCES
Agosta, F., Galantucci, S., Canu, E., Cappa, S. F., Magnani, G., Franceschi, M., ... Filippi, M. (2013). Disruption of structural connectivity along the dorsal and ventral language pathways in patients with nonfluent and semantic variant primary progressive aphasia: A DT MRI study and a literature review. *Brain and Language*, 127(2), 157–166. https://doi.org/10.1016/j.bandl.2013.06.003

Almairac, F., Duffau, H., & Herbet, G. (2018). Contralesional macrostructural plasticity of the insular cortex in patients with glioma: A VBM study. *Neurology*, 91(20), e1902–e1908. https://doi.org/10.1212/WNL.0000000000006517

Almairac, F., Herbet, G., Moritz-Gasser, S., de Champfleur, N. M., & Duffau, H. (2015). The left inferior fronto-occipital fasciculus subserves language semantics: A multilevel lesion study. *Brain Structure & Function*, 220(4), 1983–1995. https://doi.org/10.1007/s00429-014-0773-1

Ashburner, J. (2007). A fast diffeomorphic image registration algorithm. *NeuroImage*, 38(1), 95–113. https://doi.org/10.1016/j.neuroimage.2007.07.007

Bourguignon, M., Molinaro, N., & Wens, V. (2018). Contrasting functional imaging parametric maps: The mislocation problem and alternative solutions. *NeuroImage*, 169, 200–211. https://doi.org/10.1016/j.neuroimage.2017.12.033

Butefisch, C. M., Kleiser, R., Korber, B., Muller, K., Wittsack, H. J., Homberg, V., & Seitz, R. J. (2005). Recruitment of contralesional motor cortex in stroke patients with recovery of hand function. *Neurology*, 64(6), 1067–1069. https://doi.org/10.1212/01.WNL.0000154603.48446.36

Cargnelutti, E., Ius, T., Skrap, M., & Tomasino, B. (2020). What do we know about pre- and postoperative plasticity in patients with glioma? A review of neuroimaging and intraoperative mapping studies. *Neuroimage: Clinical*, 28, 102435. https://doi.org/10.1016/j.nicl.2020.102435

Carreiras, M., Seghier, M. L., Baquero, S., Estevez, A., Lozano, A., Devlin, J. T., & Price, C. J. (2009). An anatomical signature for literacy. *Nature*, 461(7266), 983–986. https://doi.org/10.1038/nature08461

Castellanos, N. P., Paul, N., Ordonez, V. E., Demuynck, O., Bajo, R., Campo, P., ... Maestu, F. (2010). Reorganization of functional connectivity as a correlate of cognitive recovery in acquired brain injury. *Brain*, 133(Pt 8), 2365–2381. https://doi.org/10.1093/brain/awq174

Catani, M. (2007). From hodology to function. *Brain*, 130(Pt 3), 602–605. https://doi.org/10.1093/brain/awm008

Catani, M., & Mesulam, M. (2008). The arcuate fasciculus and the disconnection theme in language and aphasia: History and current state. *Cortex*, 44(8), 953–961. https://doi.org/10.1016/j.cortex.2008.04.002

Celeghin, A., Diano, M., de Gelder, B., Weiskrantz, L., Marzi, C. A., & Tamietto, M. (2017). Intact hemisphere and corpus callosum compensate for visuomotor functions after early visual cortex damage. *Proceedings of the National Academy of Sciences of the United States of America*, 114(48), E10475–E10483. https://doi.org/10.1073/pnas.1714801114

Crawford, J. R., & Howell, D. C. (1998). Comparing an Individual's Test Score Against Norms Derived from Small Samples. *The Clinical Neuropsychologist*, 12(4), 482–486. https://doi.org/10.1076/clin.12.4.482.7241

Dale, A. M., & Sereno, M. I. (1993). Improved localizadon of cortical activity by combining EEG and MEG with MRI cortical surface reconstruction: A linear approach. *Journal of Cognitive Neuroscience*, 5(2), 162–176. https://doi.org/10.1162/jocn.1993.5.2.162

DeAngelis, L. M. (2001). Brain tumors. *The New England Journal of Medicine*, 344(2), 114–123.

De Benedictis, A., & Duffau, H. (2011). Brain hodotopy: From esoteric concept to practical surgical applications. *Neurosurgery*, 68(6), 1709–1723. https://doi.org/10.1227/NEU.0b013e3182124690

de Bruin, A., Carreiras, M., & Duñabeitia, J. A. (2017). The BEST dataset of language proficiency. *Frontiers in Psychology*, 8, 522. https://doi.org/10.3389/fpsyg.2017.00522

Duffau, H. (2005). Lessons from brain mapping in surgery for low-grade glioma: Insights into associations between tumour and brain plasticity. *Lancet Neurology*, 4(8), 476–486. https://doi.org/10.1016/S1474-4422(05)70140-X

Duffau, H., & Capelle, L. (2001). Functional recuperation following lesions of the primary somatosensory fields. Study of compensatory mechanisms. *Neurochirurgie*, 47(6), 557–563.

Duffau, H., Moritz-Gasser, S., & Mandonnet, E. (2014). A re-examination of neural basis of language processing: Proposal of a dynamic hodotopical model from data provided by brain stimulation mapping during picture naming. *Brain and Language*, 131, 1–10. https://doi.org/10.1016/j.bandl.2013.05.011

Duffau, H., Leroy, M., & Gatignol, P. (2008). Cortico-subcortical organization of language networks in the right hemisphere: an electrostimulation study in left-handers. *Neuropsychologia*, 46(14), 3197–3209. http://doi.org/10.1016/j.neuropsychologia.2008.07.017.

Fries, P. (2005). A mechanism for cognitive dynamics: Neuronal communication through neuronal coherence. *Trends in Cognitive Sciences*, 9(10), 474–480. https://doi.org/10.1016/j.tics.2005.08.011

Gainotti, G., Silveri, M. C., Daniele, A., & Giustolisi, L. (1995). Neuroanatomical correlates of category-specific semantic disorders: A critical survey. *Memory*, 3(3–4), 247–264. https://doi.org/10.1080/09658219508253153

Ganushchak, L. Y., Christoffels, I. K., & Schiller, N. O. (2011). The use of electroencephalography in language production research: A review. *Frontiers in Psychology*, 2, 208. https://doi.org/10.3389/fpsyg.2011.00208

Gleichgerrcht, E., Fridriksson, J., Rorden, C., Nesland, T., Desai, R., & Bonilha, L. (2016). Separate neural systems support representations for actions and objects during narrative speech in post-stroke aphasia. *Neuroimage: Clinical*, 10, 140–145. https://doi.org/10.1016/j.nicl.2015.11.013

Gramfort, A., Luessi, M., Larson, E., Engemann, D. A., Strohmeier, D., Brodbeck, C., ... Hamalainen, M. S. (2014). MNE software for processing MEG and EEG data. *NeuroImage*, 86, 446–460. https://doi.org/10.1016/j.neuroimage.2013.10.027

Grisoni, L., Dreyer, F. R., & Pulvermuller, F. (2016). Somatotopic semantic priming and prediction in the motor system. *Cerebral Cortex*, 26(5), 2353–2366. https://doi.org/10.1093/cercor/bhw026

Grutzner, C., Uhlhaas, P. J., Genc, E., Kohler, A., Singer, W., & Wibral, M. (2010). Neuroelectromagnetic correlates of perceptual closure processes. *The Journal of Neuroscience*, 30(24), 8342–8352. https://doi.org/10.1523/JNEUROSCI.5434-09.2010

Hauk, O., Johnsrude, I., & Pulvermuller, F. (2004). Somatotopic representation of action words in human motor and premotor cortex. *Neuron*, *41*(2), 301–307. https://doi.org/10.1016/s0896-6273(03)00838-9

Herbet, G., Moritz-Gasser, S., & Duffau, H. (2017). Direct evidence for the contributive role of the right inferior fronto-occipital fasciculus in non-verbal semantic cognition. *Brain Structure & Function*, *222*(4), 1597–1610. https://doi.org/10.1007/s00429-016-1294-x

Huttenlocher, J., & Lui, F. (1979). The semantic organization of some simple nouns and verbs. *Journal of Verbal Learning and Verbal Behavior*, *18*(2), 141–162.

Indefrey, P. (2011). The spatial and temporal signatures of word production components: A critical update. *Frontiers in Psychology*, *2*, 255. https://doi.org/10.3389/fpsyg.2011.00255

Indefrey, P., & Levelt, W. J. (2004). The spatial and temporal signatures of word production components. *Cognition*, *92*(1–2), 101–144. https://doi.org/10.1016/j.cognition.2002.06.001

Ius, T., Angelini, E., Thiebaut de Schotten, M., Mandonnet, E., & Duffau, H. (2011). Evidence for potentials and limitations of brain plasticity using an atlas of functional resectability of WHO grade II gliomas: towards a "minimal common brain". *NeuroImage*, *56*(3), 992–1000. https://doi.org/10.1016/j.neuroimage.2011.03.022

Jeong, J. W., Asano, E., Juhasz, C., Behen, M. E., & Chugani, H. T. (2016). Postoperative axonal changes in the contralateral hemisphere in children with medically refractory epilepsy: A longitudinal diffusion tensor imaging connectome analysis. *Human Brain Mapping*, *37*(11), 3946–3956. https://doi.org/10.1002/hbm.23287

Jung, T. P., Makeig, S., Humphries, C., Lee, T. W., Mckeown, M. J., Iragui, V., & Sejnowski, T. J. (2000). Removing electroencephalographic artifacts by blind source separation. *Psychophysiology*, *37*(02), 163–178.

Kamali, A., Flanders, A. E., Brody, J., Hunter, J. V., & Hasan, K. M. (2014). Tracing superior longitudinal fasciculus connectivity in the human brain using high resolution diffusion tensor tractography. *Brain Structure & Function*, *219*(1), 269–281. https://doi.org/10.1007/s00429-012-0498-y

Kemmerer, D., Rudrauf, D., Manzel, K., & Tranel, D. (2012). Behavioral patterns and lesion sites associated with impaired processing of lexical and conceptual knowledge of actions. *Cortex*, *48*(7), 826–848. https://doi.org/10.1016/j.cortex.2010.11.001

Kielar, A., Deschamps, T., Jokel, R., & Meltzer, J. A. (2016). Functional reorganization of language networks for semantics and syntax in chronic stroke: Evidence from MEG. *Human Brain Mapping*, *37*(8), 2869–2893. https://doi.org/10.1002/hbm.23212

Kopell, N., Ermentrout, G. B., Whittington, M. A., & Traub, R. D. (2000). Gamma rhythms and beta rhythms have different synchronization properties. *Proceedings of the National Academy of Sciences of the United States of America*, *97*(4), 1867–1872. https://doi.org/10.1073/pnas.97.4.1867

Laaksonen, H., Kujala, J., Hulten, A., Liljestrom, M., & Salmelin, R. (2012). MEG evoked responses and rhythmic activity provide spatiotemporally complementary measures of neural activity in language production. *NeuroImage*, *60*(1), 29–36. https://doi.org/10.1016/j.neuroimage.2011.11.087

Li, W., An, D., Tong, X., Liu, W., Xiao, F., Ren, J., ... Zhou, D. (2019). Different patterns of white matter changes after successful surgery of mesial temporal lobe epilepsy. *Neuroimage: Clinical*, *21*, 101631. https://doi.org/10.1016/j.nicl.2018.101631

Liljestrom, M., Kujala, J., Stevenson, C., & Salmelin, R. (2015). Dynamic reconfiguration of the language network preceding onset of speech in picture naming. *Human Brain Mapping*, *36*(3), 1202–1216. https://doi.org/10.1002/hbm.22697

Lizarazu, M., Gil-Robles, S., Pomposo, I., Nara, S., Amoruso, L., Quiñones, I., & Carreiras, M. (2020). Spatiotemporal dynamics of postoperative functional plasticity in patients with brain tumors in language areas. *Brain and Language*, *202*, 104741. https://doi.org/10.1016/j.bandl.2019.104741

Lubrano, V., Filleron, T., Demonet, J. F., & Roux, F. E. (2014). Anatomical correlates for category-specific naming of objects and actions: A brain stimulation mapping study. *Human Brain Mapping*, *35*(2), 429–443. https://doi.org/10.1002/hbm.22189

Maguire, E. A., Gadian, D. G., Johnsrude, I. S., Good, C. D., Ashburner, J., Frackowiak, R. S., & Frith, C. D. (2000). Navigation-related structural change in the hippocampi of taxi drivers. *Proceedings of the National Academy of Sciences of the United States of America*, *97*(8), 4398–4403. https://doi.org/10.1073/pnas.070039597

Makowski. (2018). The psycho package: An efficient and publishing-oriented workflow for psychological science. *Journal of Open Source Software*, *3*(22), 470. https://doi.org/10.21105/joss.00470

Makris, N., Kennedy, D. N., McInerney, S., Sorensen, A. G., Wang, R., Caviness, V. S., Jr., & Pandya, D. N. (2005). Segmentation of subcomponents within the superior longitudinal fascicle in humans: A quantitative, in vivo, DT-MRI study. *Cerebral Cortex*, *15*(6), 854–869. https://doi.org/10.1093/cercor/bhh186

Mandelli, M. L., Caverzasi, E., Binney, R. J., Henry, M. L., Lobach, I., Block, N., ... Gorno-Tempini, M. L. (2014). Frontal white matter tracts sustaining speech production in primary progressive aphasia. *The Journal of Neuroscience*, *34*(29), 9754–9767. https://doi.org/10.1523/JNEUROSCI.3464-13.2014

Maris, E., & Oostenveld, R. (2007). Nonparametric statistical testing of EEG- and MEG-data. *Journal of Neuroscience Methods*, *164*(1), 177–190.

Miozzo, M., Pulvermuller, F., & Hauk, O. (2015). Early parallel activation of semantics and phonology in picture naming: Evidence from a multiple linear regression MEG study. *Cerebral Cortex*, *25*(10), 3343–3355. https://doi.org/10.1093/cercor/bhu137

Moseley, R. L., Pulvermuller, F., & Shtyrov, Y. (2013). Sensorimotor semantics on the spot: Brain activity dissociates between conceptual categories within 150 ms. *Scientific Reports*, *3*, 1928. https://doi.org/10.1038/srep01928

Noonan, K. A., Jefferies, E., Visser, M., & Lambon Ralph, M. A. (2013). Going beyond inferior prefrontal involvement in semantic control: Evidence for the additional contribution of dorsal angular gyrus and posterior middle temporal cortex. *Journal of Cognitive Neuroscience*, *25*(11), 1824–1850. https://doi.org/10.1162/jocn_a_00442

Oldfield, R. C. (1971). The assessment and analysis of handedness: The Edinburgh inventory. *Neuropsychologia*, *9*(1), 97–113.

Oostenveld, R., Fries, P., Maris, E., & Schoffelen, J. M. (2011). FieldTrip: Open source software for advanced analysis of MEG, EEG, and invasive electrophysiological data. *Computational Intelligence and Neuroscience*, *2011*, 156869–156869. https://doi.org/10.1155/2011/156869

Payne, B. R., & Lomber, S. G. (2001). Reconstructing functional systems after lesions of cerebral cortex. *Nature Reviews. Neuroscience*, *2*(12), 911–919. https://doi.org/10.1038/35104085

Piai, V., De Witte, E., Sierpowska, J., Zheng, X., Hinkley, L. B., Mizuiri, D., ... Nagarajan, S. S. (2020). Language neuroplasticity in brain tumor patients revealed by magnetoencephalography. *Journal of Cognitive Neuroscience*, *32*, 1–11. https://doi.org/10.1162/jocn_a_01561

Piai, V., Meyer, L., Dronkers, N. F., & Knight, R. T. (2017). Neuroplasticity of language in left-hemisphere stroke: Evidence linking subsecond electrophysiology and structural connections. *Human Brain Mapping*, *38*(6), 3151–3162. https://doi.org/10.1002/hbm.23581

Piai, V., Roelofs, A., Rommers, J., & Maris, E. (2015). Beta oscillations reflect memory and motor aspects of spoken word production. *Human Brain Mapping*, *36*(7), 2767–2780. https://doi.org/10.1002/hbm.22806

Pisoni, A., Mattavelli, G., Casarotti, A., Comi, A., Riva, M., Bello, L., & Papagno, C. (2018). Object-action dissociation: A voxel-based lesion-symptom mapping study on 102 patients after glioma removal. *Neuroimage: Clinical*, *18*, 986–995. https://doi.org/10.1016/j.nicl.2018.03.022

Pulvermuller, F., Lutzenberger, W., & Preissl, H. (1999). Nouns and verbs in the intact brain: Evidence from event-related potentials and high-

frequency cortical responses. *Cerebral Cortex*, 9(5), 497–506. https://doi.org/10.1093/cercor/9.5.497

Rajapakse, J. C., Giedd, J. N., & Rapoport, J. L. (1997). Statistical approach to segmentation of single-channel cerebral MR images. *IEEE Transactions on Medical Imaging*, 16(2), 176–186. https://doi.org/10.1109/42.563663

Reid, L. B., Boyd, R. N., Cunnington, R., Rose, S. E. (2016). Interpreting intervention induced neuroplasticity with fmri: the case for multimodal imaging strategies. *Neur Plast*, 1–13.

Robles, S. G., Gatignol, P., Lehericy, S., & Duffau, H. (2008). Long-term brain plasticity allowing a multistage surgical approach to World Health Organization grade II gliomas in eloquent areas. *Journal of Neurosurgery*, 109(4), 615–624. https://doi.org/10.3171/JNS/2008/109/10/0615

Rojkova, K., Volle, E., Urbanski, M., Humbert, F., Dell'Acqua, F., & Thiebaut de Schotten, M. (2016). Atlasing the frontal lobe connections and their variability due to age and education: A spherical deconvolution tractography study. *Brain Structure & Function*, 221(3), 1751–1766. https://doi.org/10.1007/s00429-015-1001-3

Rorden, C., Karnath, H. O., & Bonilha, L. (2007). Improving lesion-symptom mapping. *Journal of Cognitive Neuroscience*, 19(7), 1081–1088. https://doi.org/10.1162/jocn.2007.19.7.1081

Roux, F., Armstrong, B. C., & Carreiras, M. (2017). Chronset: An automated tool for detecting speech onset. *Behavior Research Methods*, 49(5), 1864–1881. https://doi.org/10.3758/s13428-016-0830-1

Saarinen, T., Laaksonen, H., Parviainen, T., & Salmelin, R. (2006). Motor cortex dynamics in visuomotor production of speech and non-speech mouth movements. *Cerebral Cortex*, 16(2), 212–222. https://doi.org/10.1093/cercor/bhi099

Salmelin, R., & Sams, M. (2002). Motor cortex involvement during verbal versus non-verbal lip and tongue movements. *Human Brain Mapping*, 16(2), 81–91. https://doi.org/10.1002/hbm.10031

Sarubbo, S., De Benedictis, A., Merler, S., Mandonnet, E., Balbi, S., Granieri, E., & Duffau, H. (2015). Towards a functional atlas of human white matter. *Human Brain Mapping*, 36(8), 3117–3136. https://doi.org/10.1002/hbm.22832

Sassenhagen, J., & Draschkow, D. (2019). Cluster-based permutation tests of MEG/EEG data do not establish significance of effect latency or location. *Psychophysiology*, 56(6), e13335. https://doi.org/10.1111/psyp.13335

Schlaug, G., Marchina, S., & Norton, A. (2009). Evidence for plasticity in white-matter tracts of patients with chronic Broca's aphasia undergoing intense intonation-based speech therapy. *Annals of the New York Academy of Sciences*, 1169, 385–394. https://doi.org/10.1111/j.1749-6632.2009.04587.x

Shimizu, T., Hosaki, A., Hino, T., Sato, M., Komori, T., Hirai, S., & Rossini, P. M. (2002). Motor cortical disinhibition in the unaffected hemisphere after unilateral cortical stroke. *Brain*, 125(Pt 8), 1896–1907. https://doi.org/10.1093/brain/awf183

Spironelli, C., Manfredi, M., & Angrilli, A. (2013). Beta EEG band: A measure of functional brain damage and language reorganization in aphasic patients after recovery. *Cortex*, 49(10), 2650–2660. https://doi.org/10.1016/j.cortex.2013.05.003

Taulu, S, & Simola, J. (2006). Spatiotemporal signal space separation method for rejecting nearby interference in MEG measurements. *Physics in Medicine & Biology*, 51(7), 1759.

Thompson-Schill, S. L., D'Esposito, M., & Kan, I. P. (1999). Effects of repetition and competition on activity in left prefrontal cortex during word generation. *Neuron*, 23(3), 513–522. https://doi.org/10.1016/s0896-6273(00)80804-1

Tohka, J., Zijdenbos, A., & Evans, A. (2004). Fast and robust parameter estimation for statistical partial volume models in brain MRI. *NeuroImage*, 23(1), 84–97. https://doi.org/10.1016/j.neuroimage.2004.05.007

Tranel, D., Adolphs, R., Damasio, H., & Damasio, A. R. (2001). A neural basis for the retrieval of words for actions. *Cognitive Neuropsychology*, 18(7), 655–674. https://doi.org/10.1080/02643290126377

Traut, T., Sardesh, N., Bulubas, L., Findlay, A., Honma, S. M., Mizuiri, D., ... Tarapore, P. E. (2019). MEG imaging of recurrent gliomas reveals functional plasticity of hemispheric language specialization. *Human Brain Mapping*, 40(4), 1082–1092. https://doi.org/10.1002/hbm.24430

Uhlhaas, P. J., Liddle, P., Linden, D. E. J., Nobre, A. C., Singh, K. D., & Gross, J. (2017). Magnetoencephalography as a tool in psychiatric research: Current status and perspective. *Biological Psychiatry: Cognitive Neuroscience and Neuroimaging*, 2(3), 235–244. https://doi.org/10.1016/j.bpsc.2017.01.005

Van Veen, B. D., van Drongelen, W., Yuchtman, M., & Suzuki, A. (1997). Localization of brain electrical activity via linearly constrained minimum variance spatial filtering. *IEEE Transactions on Biomedical Engineering*, 44(9), 867–880. https://doi.org/10.1109/10.623056

Vassal, M., Le Bars, E., Moritz-Gasser, S., Menjot, N., & Duffau, H. (2010). Crossed aphasia elicited by intraoperative cortical and subcortical stimulation in awake patients. *Journal of Neurosurgery*, 113(6), 1251–1258.

Varela, F., Lachaux, J. P., Rodriguez, E., & Martinerie, J. (2001). The brainweb: Phase synchronization and large-scale integration. *Nature Reviews. Neuroscience*, 2(4), 229–239. https://doi.org/10.1038/35067550

Vigliocco, G., Vinson, D. P., Druks, J., Barber, H., & Cappa, S. F. (2011). Nouns and verbs in the brain: A review of behavioural, electrophysiological, neuropsychological and imaging studies. *Neuroscience & Biobehavioral Reviews*, 35(3), 407–426. https://doi.org/10.1016/j.neubiorev.2010.04.007

Vinson, D. P., Vigliocco, G., Cappa, S., & Siri, S. (2003). The breakdown of semantic knowledge: Insights from a statistical model of meaning representation. *Brain and Language*, 86(3), 347–365. https://doi.org/10.1016/s0093-934x(03)00144-5

Vorwerk, J., Cho, J. H., Rampp, S., Hamer, H., Knosche, T. R., & Wolters, C. H. (2014). A guideline for head volume conductor modeling in EEG and MEG. *NeuroImage*, 100, 590–607. https://doi.org/10.1016/j.neuroimage.2014.06.040

Walker, D. G., & Kaye, A. H. (2003). Low grade glial neoplasms. *Journal of Clinical Neuroscience*, 10(1), 1–13. https://doi.org/10.1016/s0967-5868(02)00261-8

Watson, C. E., Cardillo, E. R., Ianni, G. R., & Chatterjee, A. (2013). Action concepts in the brain: An activation likelihood estimation meta-analysis. *Journal of Cognitive Neuroscience*, 25(8), 1191–1205. https://doi.org/10.1162/jocn_a_00401

Weiss, S., & Mueller, H. M. (2012). "Too many betas do not spoil the broth": The role of beta brain oscillations in language processing. *Frontiers in Psychology*, 3, 201. https://doi.org/10.3389/fpsyg.2012.00201

Wright, P., Stamatakis, E. A., & Tyler, L. K. (2012). Differentiating hemispheric contributions to syntax and semantics in patients with left-hemisphere lesions. *The Journal of Neuroscience*, 32(24), 8149–8157. https://doi.org/10.1523/JNEUROSCI.0485-12.2012

Zhang, N., Xia, M., Qiu, T., Wang, X., Lin, C. P., Guo, Q., ... Zhou, L. (2018). Reorganization of cerebro-cerebellar circuit in patients with left hemispheric gliomas involving language network: A combined structural and resting-state functional MRI study. *Human Brain Mapping*, 39(12), 4802–4819. https://doi.org/10.1002/hbm.24324